



THE UNIVERSITY *of* EDINBURGH

Edinburgh Research Explorer

Measurement of Platform Conductor Preload in Streamlining the Life Extensions of Ageing Offshore Wells

Citation for published version:

Ramasamy, R, Ibrahim, Z, Chai, HK & Chau, TF 2017, 'Measurement of Platform Conductor Preload in Streamlining the Life Extensions of Ageing Offshore Wells', *Applied Ocean Research*, vol. 65, pp. 12–22. <https://doi.org/10.1016/j.apor.2017.03.004>

Digital Object Identifier (DOI):

[10.1016/j.apor.2017.03.004](https://doi.org/10.1016/j.apor.2017.03.004)

Link:

[Link to publication record in Edinburgh Research Explorer](#)

Document Version:

Peer reviewed version

Published In:

Applied Ocean Research

General rights

Copyright for the publications made accessible via the Edinburgh Research Explorer is retained by the author(s) and / or other copyright owners and it is a condition of accessing these publications that users recognise and abide by the legal requirements associated with these rights.

Take down policy

The University of Edinburgh has made every reasonable effort to ensure that Edinburgh Research Explorer content complies with UK legislation. If you believe that the public display of this file breaches copyright please contact openaccess@ed.ac.uk providing details, and we will remove access to the work immediately and investigate your claim.



Measurement of Platform Conductor Preload in Streamlining the Life Extensions of Ageing Offshore Wells

Ramesh Ramasamy^{a,*}, Zainah Ibrahim^a, Hwa Kian Chai^b, Ting Fai Chau^c

^aFaculty of Engineering, University of Malaya, 50603 Kuala Lumpur, Malaysia.

^bSchool of Engineering, University of Edinburgh, EH8 9YL United Kingdom.

^cAzakti Energy Ltd., Covent Garden, London WC2H 9JQ, United Kingdom.

*Corresponding Author, ramesh.ramasamy@siswa.um.edu.my; ramasamy.ramesh@gmail.com

ABSTRACT

The life extension of ageing oil wells is becoming an ever more crucial part of an operator's activities in recent years, mainly due to slumping oil price which discourages new exploration and the potential extended operation of some older fields with sufficient producing capacity still remaining. The conductor forms one of the primary structural components of wells and its deterioration over time warrants immediate integrity assessment and rehabilitation plans. The construction residual loading or preloads on the conductor are calculated as per standard guidelines and by analytical means during its design and installation phase, but may not be realistic when assessing aged conductors, due to the high levels of over-conservatism built in to address the various uncertainties during the well drilling phase, hence a more practical means of evaluating this residual load is required in carrying out the integrity assessments. This paper presents the novel use of ultrasonic based non-destructive technique (NDT) to measure the conductor preload by observing the travel time of the longitudinal critical refracted (LCR) waves and employing the acoustoelastic method to determine the structural stresses. The measurement of the time of flight (TOF) of this wave component is evaluated from the signals measurement under a range of preload stresses induced into the specimen, and the acoustoelastic calibration curve is obtained as a result, for various section geometries and dimensions. Numerical analyses are also carried out to correlate and validate the magnitude order of the acoustoelastic constant of typical conductor steel grade (Grade-B). These are in good agreement with each other and can be a very reliable tool for the on-site preload measurements during oil well integrity assessment. This measurement of conductor preload results in minimising any associated uncertainties, assumptions and the corresponding over-conservatisms carried over from the design stage, hence streamlining the repair and rehabilitation strategies to the most critical well-conductor groups in the field, thus significantly reducing the costs and resources for operators in extending life of aged wells.

Keywords: Conductor Preload; Well Integrity; Life Extension; Acoustoelasticity

Highlights:

- This work explains the criticality of platform conductor assessment in ageing well integrity;
- Conductor preload plays an important role towards calculation of preload stresses, in addition to the environmental and operating loads, and are commonly over-estimated;
- Accurate prediction of the conductor preload will help streamline categorisation for repairs, potentially saving millions in premature repair cost and other resources for each well;
- This work describes development of an ultrasonic based measurements of conductor preload, implementing the acoustoelastic method and time of flight (TOF) of the longitudinal critical refracted (LCR) wave component;
- Laboratory tests are carried out to obtain specific material calibration curves, validated by numerical analyses, and can be used to obtain traditionally hard-to-determine axial preload value on conductors;
- The proposed method has great potential in quantitative integrity assessment and reliable life extension activities for ageing wells located particularly in matured shallow water fields.

INTRODUCTION

Ageing oil wells, typically in their 30s to 40s or more have long exceeded their calculated design life, or approaching the end of field life. Some of the oldest fields in the world, such as those in the Persian Gulf, North Sea or South East Asia are primarily located in the shallow to intermediate water depth and the platform conductors are very predominant feature in the well constructions. The wellhead platform towers (WHPT) popular in these fields, shown in Figure 1 typically consist of several conductors and casing systems to support wellheads either for producing or other operations such as water injections.



Figure 1 – Typical Ageing WHPT in Shallow Water Fields [1]

The common constructions schematics of these wells are shown in Figure 2, highlighting the wellhead consisting of the low and high pressure housings being supported by the conductor, surface casing and intermediate casings. The annular spaces between these different sized pipes are separated by layers of cement to centralise these pipes and to consolidate the well structure together for load redistribution. During the drilling phase, the drilling mud can also be found in some of these annuli to keep the well integrity in-place and to help with recirculating throughout the drilling activity. As the conductor will be the first barrier installed, the subsequent installation will impart loads onto the conductor, once the annular cements starts to set in each annulus, adjacent of the casings. The wellhead, connects every subsequent casing inside the well through spools and the wellhead itself can be designed to either solely sit on top on the surface casing or on both the surface casing and the conductor by some load sharing mechanism on deeper water fields and heavier blowout preventer (BOP) during drilling.

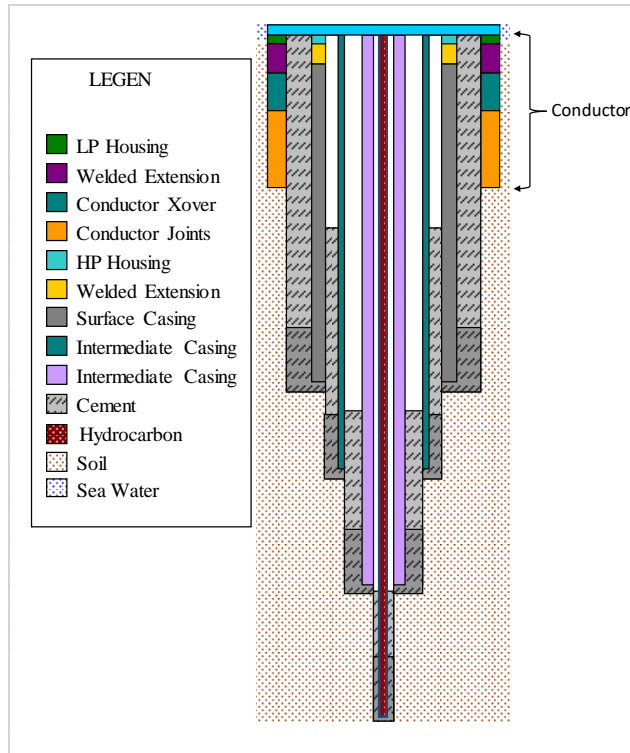


Figure 2 – Common Well Construction Schematics

The evaluation of the conductor loads is conventionally carried out based on methods recommended in [3] and [4], with the allowable criteria as stipulated in [5], and based on the well construction sequence, as shown in Table 1 for a 30in conductor in a shallow water well with a surface tree configuration.

Table 1 – Typical Well Construction Sequence and Associated Durations

Stage	Activity	Duration (Days)
1	Drilling of 36in hole, installing the 30in conductor and cementing the outside annulus top the seabed.	N/A
2	Drilling of 17in hole for 13-3/8in surface casing.	5
3	13-3/8in Surface casing (with wellhead) hung off, and cementing of its outside annulus.	2
4	Running of BOP and installing on wellhead.	1
5	Drilling of 12in hole for the 9-5/8in inner casing	10
6	9-5/8in Inner casing hung off and cementing of its outside annulus.	5
7	Drilling of 5in hole for the 3-1/2in tubing, and installing packer downhole.	5
8	Running tubing into packer and centralising cementing.	2
9	Removing BOP and Installing Surface Tree.	1

The properties for the conductor, casing strings[6] and standard topside equipment are shown in Table 2. The major uncertainties involved during drilling campaigns are the quality of the cement bond achieved between the conductor-casing-soil interfaces at each annulus and the bottom soil bearing of the strings at their set depths. In a conservative design scenario, the absence of bottom soil bearing will result in the dependence on the annuli cement bond, and larger load transfer into the conductor.

Although this is a reasonable assumption during design stage, in an aged system where the prime objective is to prolong productions, these over-conservatisms and reserve factors have to be minimised or completely removed, leading to the requirement for further rationalisation.

Table 2 – Well Component Properties

Conductor, Casings, Tubing						
Type	Outer Diameter		Weight		Yield Strength	
	in	mm	lb/ft	kg/m	ksi	MPa
30in	30	762	272	405	35.5	244
13-3/8in	13.375	340	68	101	55	379
9-5/8in	9.625	244	47	70	75	517
3-1/2in	3.5	89	9.2	13.7	80	551
Topside Equipment						
Type	Weight					
	kips		Te			
Wellhead	2.2		1.0			
BOP	13.2		6.0			
Surface Tree	8.8		4.0			

ANALYTICAL METHODS

Conductor Preload Calculation

The deterministic closed-form evaluation of the axial loading at the top of the conductor, based on the information provided in the previous section can be carried out considering the parallel springs analogy [4][3], and is shown in Figure 3, where each conductor/casing can be viewed as a linear axial spring arranged in parallel to share the common topside load and the weights of each other under the cemented situations. The strings weights will be reduced to about 75% under the buoyancy of the Class-G cement slurry in an unset condition. Once the cement sets, the strings will be held in place and its weight will be transferred to the adjacent string, conductor or sidewalls of the drilled hole.

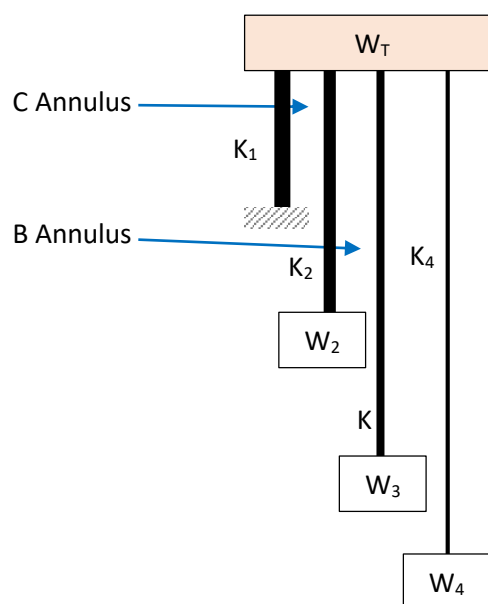


Figure 3 – Simplified Well Structural Layout

The axial stiffnesses of the conductor (K_1), surface casing (K_2), inner casing (K_3) and the tubing (K_4) are derived by the axial stiffness evaluations based on their effective free lengths down to the cemented elevations, or their full set depths if no cement is present inside that specific annulus. The topside equipment weights (W_T) consists of wellhead, surface tree/BOP, and the casing string weights ($W_1 - W_4$) are the individual string weights under the buoyant effect of the annuli cement. The intermediate stage where the presence of the drilling mud inside these annuli can be omitted due to their constant circulation and replacement with cement immediately after the drilling and installation of each string. The conductor is set to a certain depth with full direct soil bearing, or indirectly achieved through a reasonable cement job. For an ideal scenario where full cementing is assumed in both the C-annulus and B-annulus up to the surface, and for the worst case scenario with absolutely no cement present in both the annuli (possible in an aged well), a permutation of cement elevation, or top of cement (TOC) scenario is generated and listed in Table 3, with a range of cement shortfall.

Table 3 – Permutations of Annular Cement Shortfall Scenario

Case	C-Annulus	Case	B-Annulus
	depth (or length) below wellhead, m		depth (or length) below wellhead, m
C1	0	B1	0
C2	5	B2	5
C3	15	B3	15
C4	50	B4	50
C5	100	B5	100
C6	None ¹	B6	None ¹
Note: 1. No cement inside annulus			

The expression for determining the most conservative preload (upper bound) on the conductor (F_1) specifically can be derived to be as shown in Equation 1, at the final stage of drilling when the surface tree is being installed.

$$F_1 = W_T + W_2 + \left(\frac{K_1}{K_1 + K_2} \right) W_3 + \left(\frac{K_1}{K_1 + K_2 + K_3} \right) W_4$$

Equation 1

The weights W_2 to W_4 are calculated considering the buoyant effect of the annular cement and the corresponding axial stiffness for a specific string (K_i) is calculated based on the elastic modulus (E), effective free span length or un-cemented length, $L_{eff,i}$ from the wellhead and the respective string cross sectional area (A_i), as shown in Equation 2.

$$K_i = \frac{E \cdot A_i}{L_{eff,i}}$$

Equation 2

This will result in a total of 36 possible TOC scenarios, which will produce a range of conductor preload values calculated, as shown in Figure 4, from fully cemented annuli to un-cemented annuli scenario. The evaluated preloads, for both the conductor and the surface casing are compressive in nature, despite its positive values, and acts at the top end of these pipes. The presence of this spectrum of possible combinations of annular TOC can result in this wide range of preload values, with another extreme possibility of the surface casing weight solely supported by the conductor, shown as the upper bound.

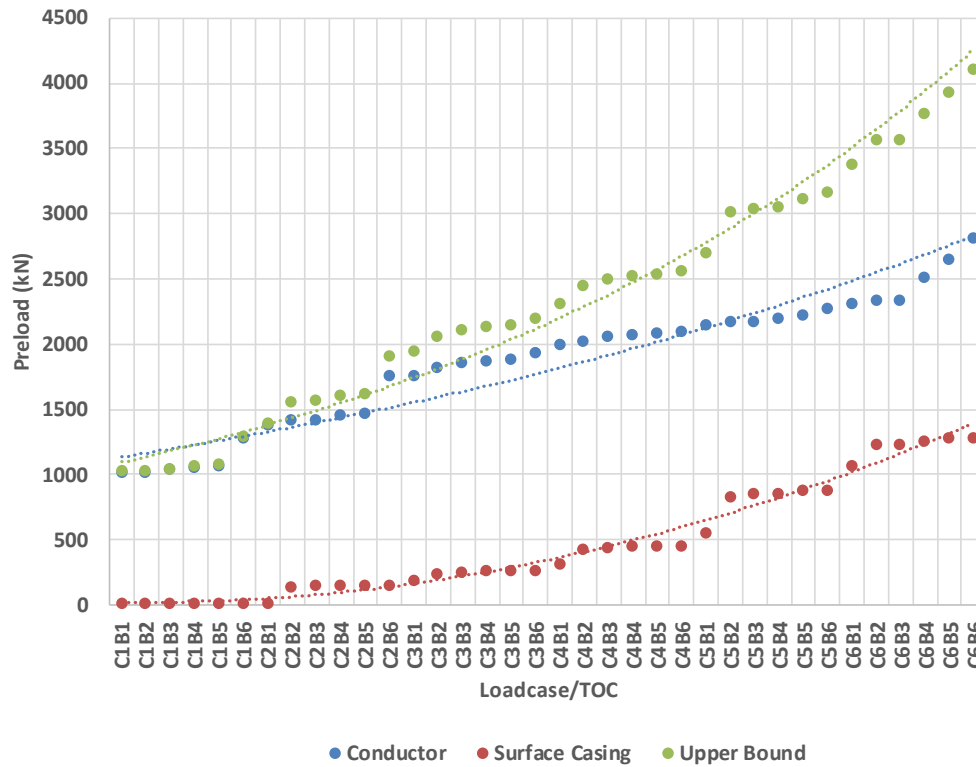


Figure 4 – Calculated Preload

Conductor Stress Analysis

The metocean data obtained from the oilfields can be used to compute the bending distributions of the conductor and casing arrangements for the nominal as-built well by means of numerical analyses, considering the current and waves, with the appropriate representations of the nonlinear pipe-soil interactions, conductor supporting guides, centralisations and thermomechanical conditions (for producer wells).

The commercial finite element package ABAQUS [8] is used to solve this global model, consisting of a pipe-in-pipe construction, nonlinear pipe-soil elements and gap contacts to represent the guides. The current and wave forces are applied using the AQUA module with the hydrodynamic coefficients stipulated in [5].

For a 100-years return period conditions, with maximum surface current of 1.5m/s, maximum wave height of 8.5m over a period of 9s, will result in the bending moment distribution as shown in Figure 5. This indicates the maximum bending moment at the splash zone (defined as $\pm 2m$ from mean sea level, MSL) to be approximately 240kNm, with the absolute maximum occurring at the seabed (350kNm).

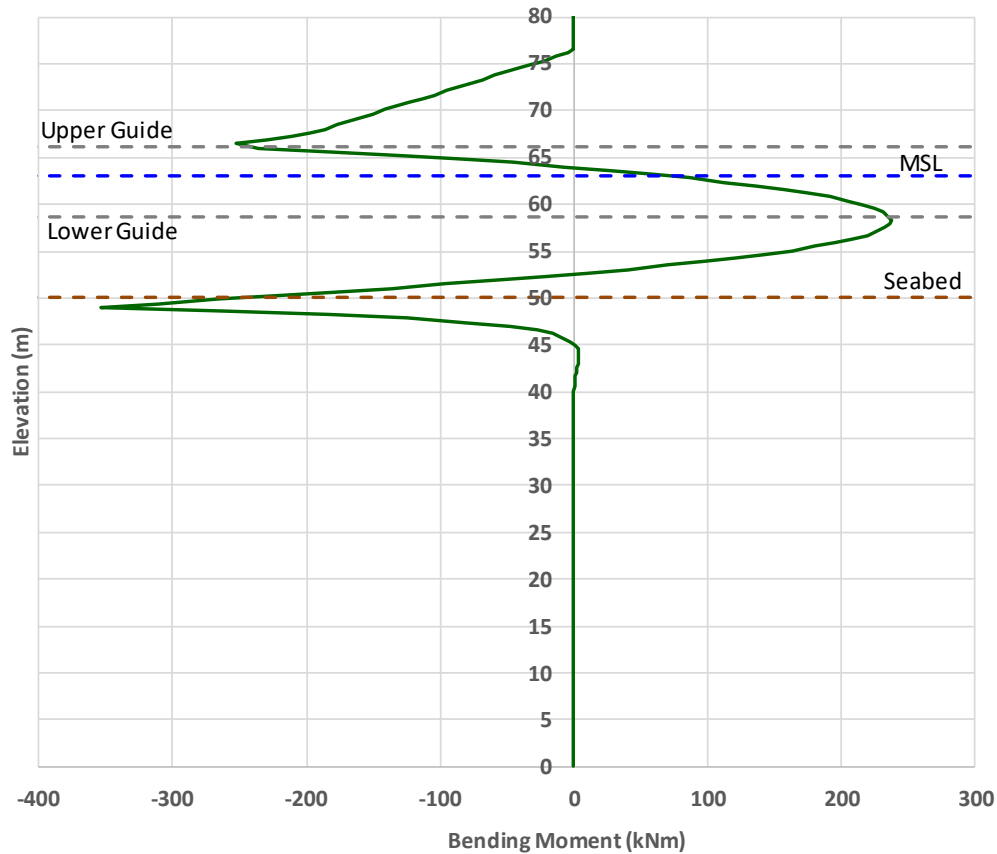


Figure 5 – Bending Moment Distribution on Conductor

The resulting total stress (σ_x) can be calculated for the bending moment (M_x) at elevation- x , axial load ($F_x = F_1 + W_x$, where W_x is the segment weight above the elevation being considered) and the sectional modulus (z_x) and cross section area (A_x) as follows:

$$\sigma_x = \frac{F_x}{A_x} + \frac{M_x}{z_x}$$

Equation 3

For the worst case conductor preload (Figure 4) and the maximum bending, the maximum stress utilisation of about 0.5 of the yield strength is evaluated on the nominal as-built pipe section at the seabed, and 0.4 at the splash zone region. The wall loss due to the aqueous corrosion on the conductor, which has been reported to be as much as 60% of the nominal section[1] and occurs at the splash zone. This can result in exceedance in yield stress utilisation ranging from 0.9 to 1.1 at these sections, with risks of catastrophic failures. However, due to the conservative value of preload estimated, these stresses are seemingly excessive and often result in unnecessary repairs on some conductors.

Integrity Assessment and Rationalisation

In an ageing well, several degradation mechanisms exist, and resulting in the deterioration of the metallic and cementitious mediums[7]. The aqueous corrosion resulting from seawater on the outside of the conductor and the hydrocarbon flowing on the inside of the production casing or tubing can interact with each other on poorly designed or poorly maintained wells, and resulting cracking. This subsequently will result in spalling of the cement due to the overstressing from the volumetric

expansion of the corrosion product exerting compressive stresses against the cement at the interfaces [8][10]. The loss of significant portions of cement inside the annuli will result in the redistribution of the preload on the conductor and casings. Other forms of deteriorations which may exist on aged wells such as slumping or collapse of surface casing downhole in the absence of reasonable TOC can also cause changes in the preloads. The proposed method of monitoring the critical splash zone region, due to its excessive corrosion and high magnitude of bending is being considered as several inspections of conductor sections below the splash zone have shown very little wall loss[1] mainly due to cathodic protections and the indirect protection by marine growth. The presentation of the splash zone region stresses for each preload from the range of preloads evaluated is shown in Figure 6 against a range of remaining minimum circumferential wall thicknesses, and provides a traffic-light guideline for operators to categorise the wells for repairs based on their criticality. The criteria used, based on API [5] are highlighted as green (0.6), yellow (0.8) and red (≥ 1) in this plot and help identify the well being assessed as either fit for continued operation, to be continuously monitored or to be immediately shut-down for repairs, respectively. The tentative upper and lower bounds of the calculated preloads envelope the integrity states of these conductors, and its crucial to get the correct or realistic preload identified prior to pin pointing the wells within this plot, as indicated in the plot.

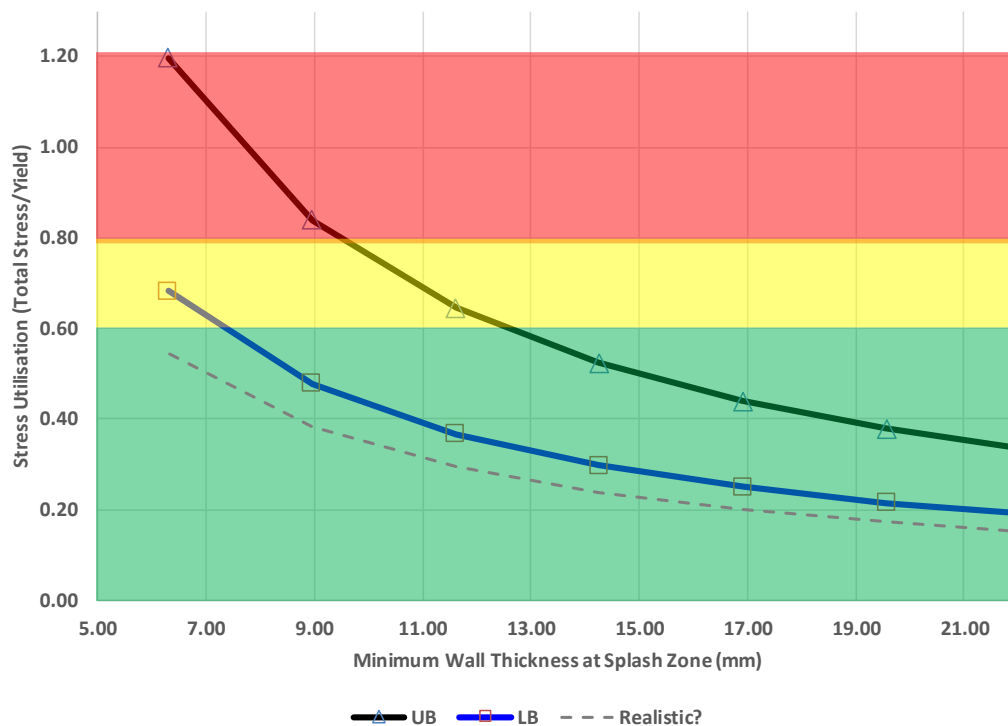


Figure 6 –Conductor Integrity Guideline Plot Showing Splash Zone Region Stress

Based on surveys carried out [1][2], some of the conductors with remaining wall thickness of < 8mm are still operating without any problems, thus raising the question on the validity of the calculated preloads for integrity assessment. This presents a complex situation where the lack of maintenance and relevant records deter the assessment of aged conductor effectively and realistically, without excessive over-conservatism in the picture. An on-site inspection method is therefore required to effectively measure and evaluate the existing preload at the top of the conductor in its current state. This can then be used to determine the stresses at the splash zone region and the categorisation of conductors can be carried out to facilitate repair and rehabilitation strategies for the corresponding life extension programme.

ULTRASONIC MEASUREMENT METHOD

Brief Introduction

The research carried out in this paper has investigated, designed and developed the ultrasonic based method to be the robust and practical method to measure the conductor preload effectively. This method is novel to the offshore industry, particularly in measuring the conductor preload for integrity assessment and life extension activities. The ultrasonic based method is also a completely non-destructive technique with fast turnaround time for results presentation in the field, with other advantages such as portability and compliance to the health and safety directives.

This paper details the development of the ultrasonic technique using the longitudinal critically refracted (LCR) wave which is developed and tested in the laboratory, implementing the acoustoelastic methods, to establish the material calibration curve, backed up with numerical validation

The acoustoelastic technique [11][12][13], in general, relies on the fact that the wave propagation speed through any isotropic medium is affected by its planar stress states, and is proportional to its stress state by a material constant. If V is the propagation speed recorded in a stressed body, and V_0 being the nominal speed in un-stressed conditions, σ being the axial planar stress and material constant (or acoustoelastic constant) K , then the linear relationship governing this behaviour can be expressed as shown in Equation 4 to Equation 6.

$$\frac{V - V_0}{V_0} = K \cdot \sigma$$

Equation 4

$$V_0 = \sqrt{\frac{\lambda + 2\mu}{\rho}}$$

Equation 5

Where λ and μ are second order elastic constants of the steel specimen, given by:

$$\lambda = \frac{\nu E}{(1 + \nu)(1 - \nu)} ; \mu = \frac{E}{2(1 + \nu)}$$

Equation 6

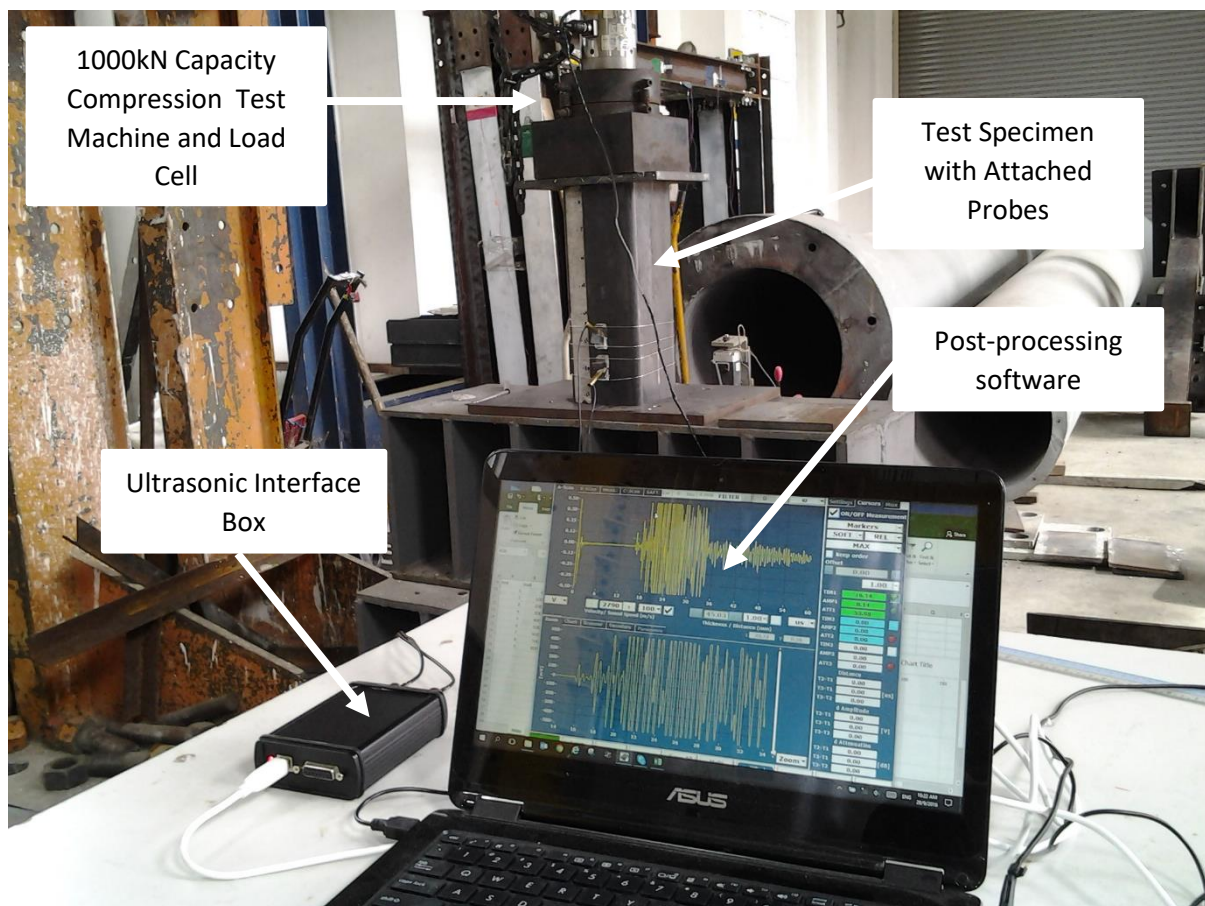
And E , ν , ρ are the specimen material elastic modulus, Poisson's ratio and nominal density respectively.

The LCR waves are also more reliable in measurement of the conductor preload since it is a subsurface wave travelling beneath the specimen outer surface (at approximately 2mm beneath surface for a 5MHz probe) and is able to penetrate through coatings and light corrosions, similar to a standard wall thickness probe or a flaw probe used widely in the offshore sector.

In the case of the conductor, the preload is the longitudinal force, which results in the longitudinal compressive stress, therefore measurement of the wave propagating along the conductor elevation can be carried out to determine the residual stress. This preload stress will be the resultant of all combinations of the in-place conditions and deteriorations of the pipe, cement and other defects.

Laboratory Setup and Testing

The setup of the ultrasonic system is shown in Figure 7 (and schematically in Figure 8) highlighting the typical conductor material, Grade-B (35ksi or 244MPa) steel test specimen consisting of, in this case, a square hollow section SHS 150mm (Width & Breadth) x 6mm (Thick) x 400 (Long), with the probes strapped around it, placed under a 1000kN capacity compression test machine with a load cell, and connected to the PC based processing software through an ultrasonic interface box (containing the pulse transmitter and receiver). The transmitting and receiving probes are fixed with Poly Methyl Methacrylate (PMMA) or more commonly known as acrylic or plexi-glass with the angle of 28° to generate the predominantly LCR subsurface waves in steel as estimated by Snell's Law. The interface box with 100kHz sampling rate is deemed adequate in capturing the TOF of the propagating ultrasonic wave from the transmitter to the receiver at each load increment, up to the material yield limit. The loading is held in place at each step to record the wave amplitudes and travel time for processing to obtain the TOF. The probes are held in place at a fixed spacing (X), depending on available access on the specimen, to enable calculation of the LCR average wave speed from the measured TOF. This can be done by means of simple wire straps or specifically engineered clamps. To account for the uncertainties of the specimen material parameters (from different vendors/manufacturers) which may result in a range of plexi-glass angle (26° to 30°), a curved bottom face is machined on the wedges used during the test to enable adjustments to achieve the effective angle to obtain the most prominent LCR wave signal by rocking it back and forth.



(a)

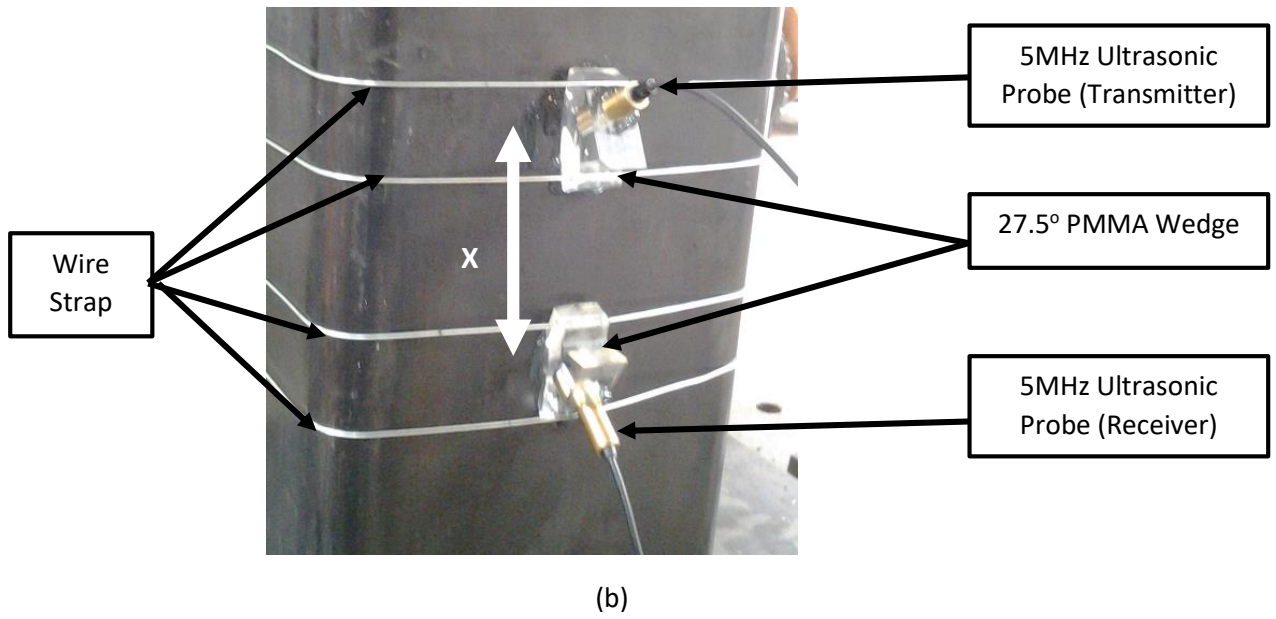


Figure 7 – (a) Ultrasonic Preload Inspection Setup, (b) Detailed View on Probe Attachments

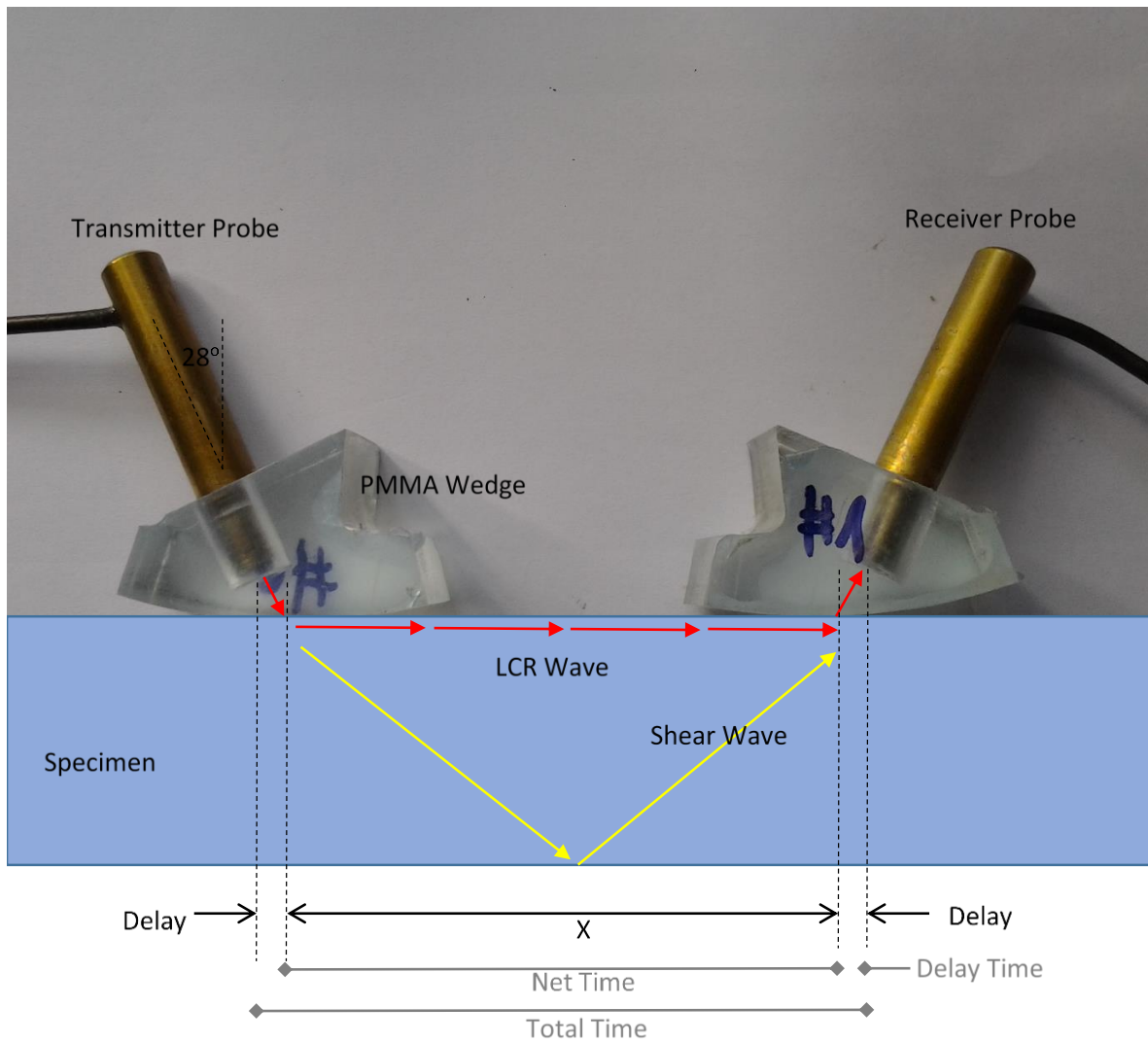


Figure 8 – Ultrasonic Wave Travel Path and Time Measurements

The material properties for the specimen and wedge used in this research are presented in Table 4.

Table 4 – Material Properties

Parameters	ρ (kg/m ³)	E (GPa)	ν (-)	Compression Wave Speed (m/s)
Specimen (Carbon Steel, Grade B)	7950	207	0.3	5920
PMMA Wedge	1100	4	0.4	2792

The wave recorded wave propagation over time from the zero stress state and every stress step are extracted (shown in Figure 9) and assessed to evaluate the individual TOF from the total travel time as being the net time taken for the wave to travel from the transmitter to the receiver in the specimen. Care must also be taken to ensure only the LCR wave signal is used for the TOF evaluations, by checking the consistency of the wave peaks at the receiver probe when the receiver probe is moved back and forth. The probes, since spaced at a known distance from each other (in this case, $X = 50\text{mm}$) will provide the necessary information to calculate the value of V at each stress state, i.e. $V = X/\text{TOF}$ m/s. The nominal LCR speed, V_0 is approximately 5920m/s in carbon steel based on measurements on a calibrated standard steel block, and can also be calculated based on exact elastic properties, and is described in detail in [16]. The measured value in this test shows a value of 5939m/s, and is within acceptable limit, with <0.5% deviation.

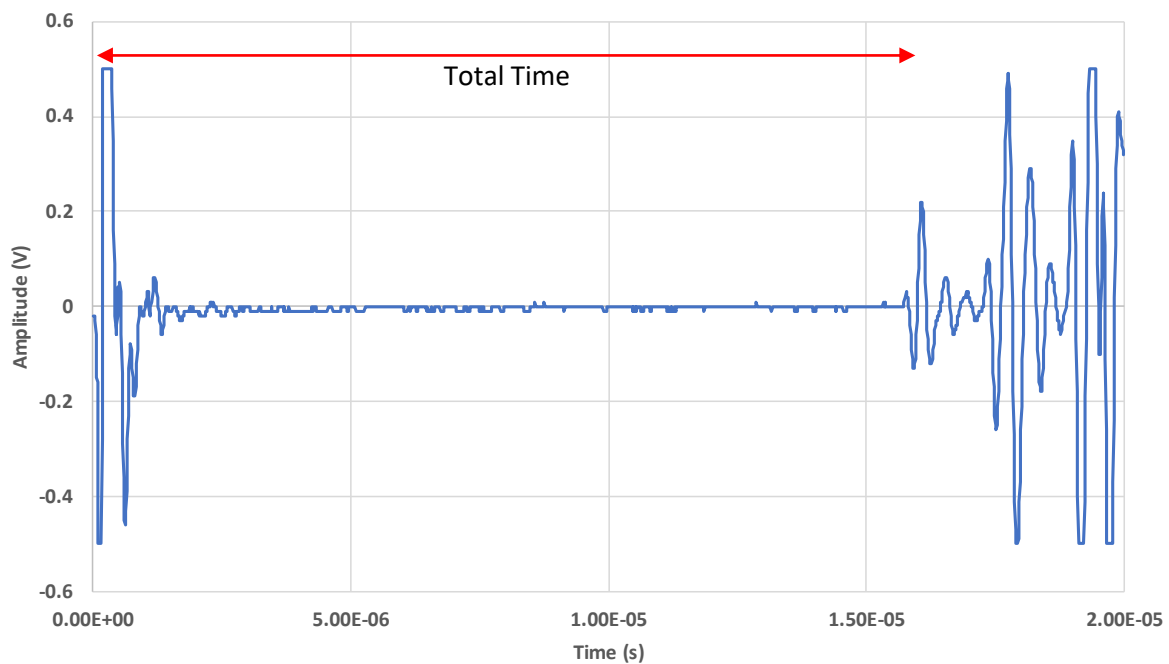


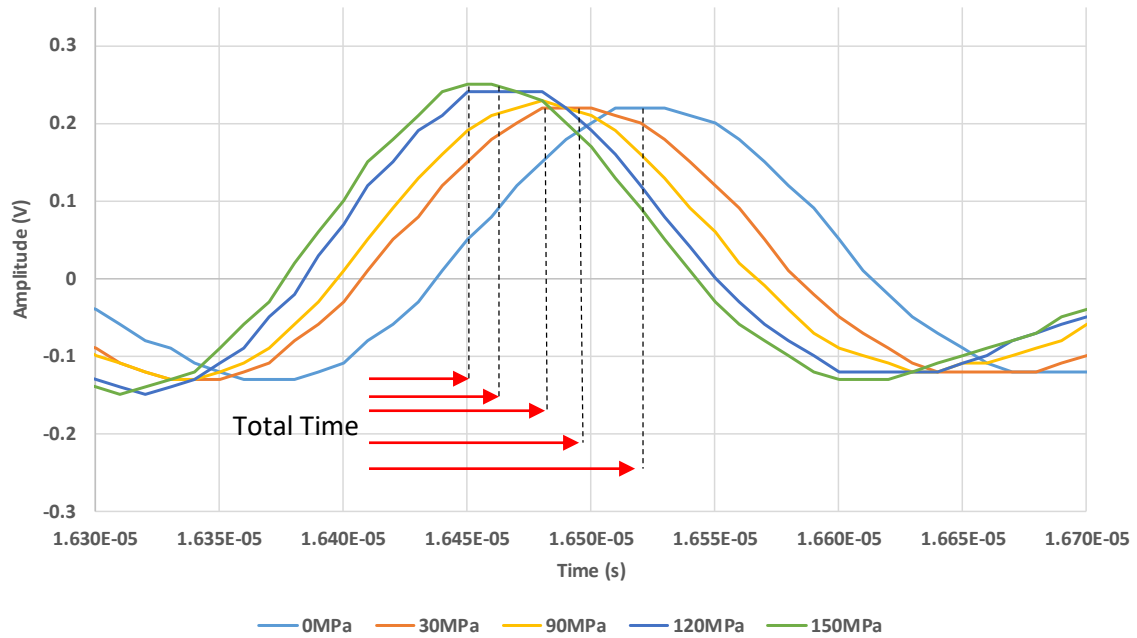
Figure 9 - Recorded Ultrasonic Wave Propagation Over Time for Zero Stress (Initial State)

Due to the fact that the wave travels from the transmitter probe, through the PMMA medium, into the steel specimen and back through the receivers' side of PMMA wedge before being picked up by the receiver probe (as shown in Figure 8), there exist a small time delay which must be accounted for to evaluate the TOF, such that $\text{TOF} = \text{Total Time} - \text{Time Delay}$. The time delay is defined as the LCR wave travel time inside the wedge material with a different speed (2792m/s, Table 4) before travelling inside the steel specimen. In this specific case, the design and construction of the wedges produces a

time delay of about $8.13\mu\text{s}$ (or 22.6mm total travel path in both transmitting and receiving wedges). The recorded wave signals for the selected load increments on the 150mm x 6mm SHS specimen is shown in Figure 10 (a), with the detailed view of the LCR incident at receiver wedge in (b).



(a)



(b)

Figure 10 – (a) Overview of Recorded Waveform, (b) Zoom-In View Showing Wave Peaks of Interest

The TOF is calculated for each load increment on the specimen, and the resulting curve relating the wave speed to the stress being applied (Equation 4) can be generated, and is shown in Figure 11.

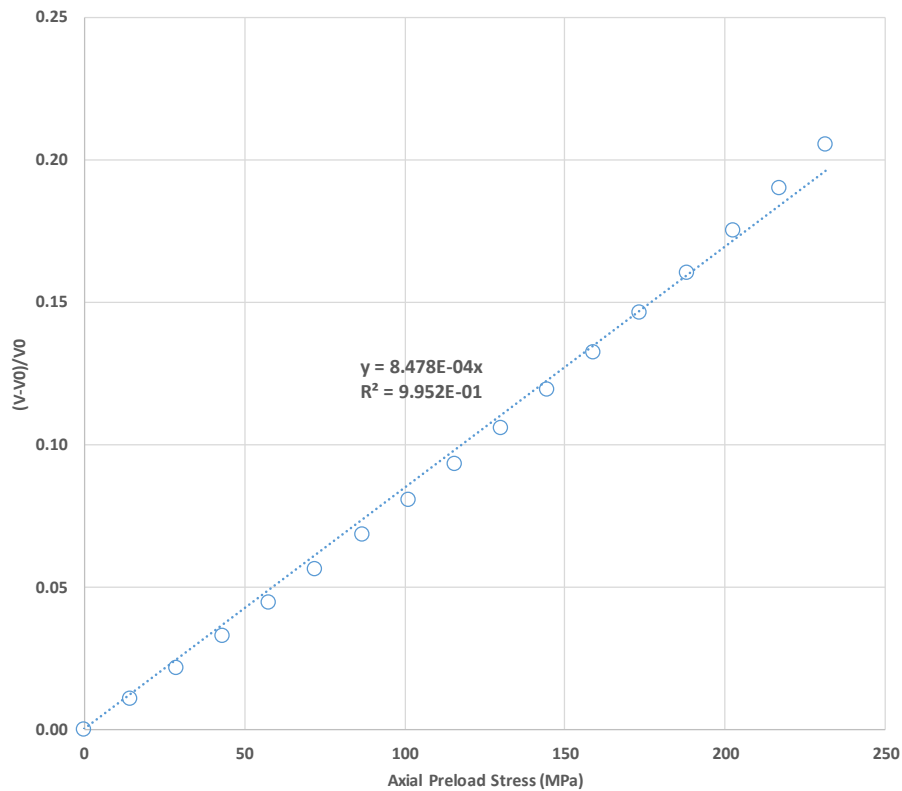


Figure 11 – Laboratory Calibration of Acoustoelastic Constant for Grade-B 150mm x 3mm SHS

Similar steps are also carried out on various circular and square hollow sections to ascertain the section/shape independence on the acoustoelastic constant, and is shown in Figure 12, with the acoustoelastic constant results tabulation in Table 5 with the associated line fitting accuracy (R^2). The nominal value of the acoustoelastic constant of carbon steel is experimentally determined to be approximately $8.5 \times 10^{-4} \text{ MPa}^{-1}$, although the larger section of SHS 200 x 10 shows a slight deviation by about 8% which is expected mainly due to insufficient points at higher stress regions due to limitation of the test machine capacity which could only impart a maximum of 1000kN or 130MPa, short of the maximum allowable of 244MPa.

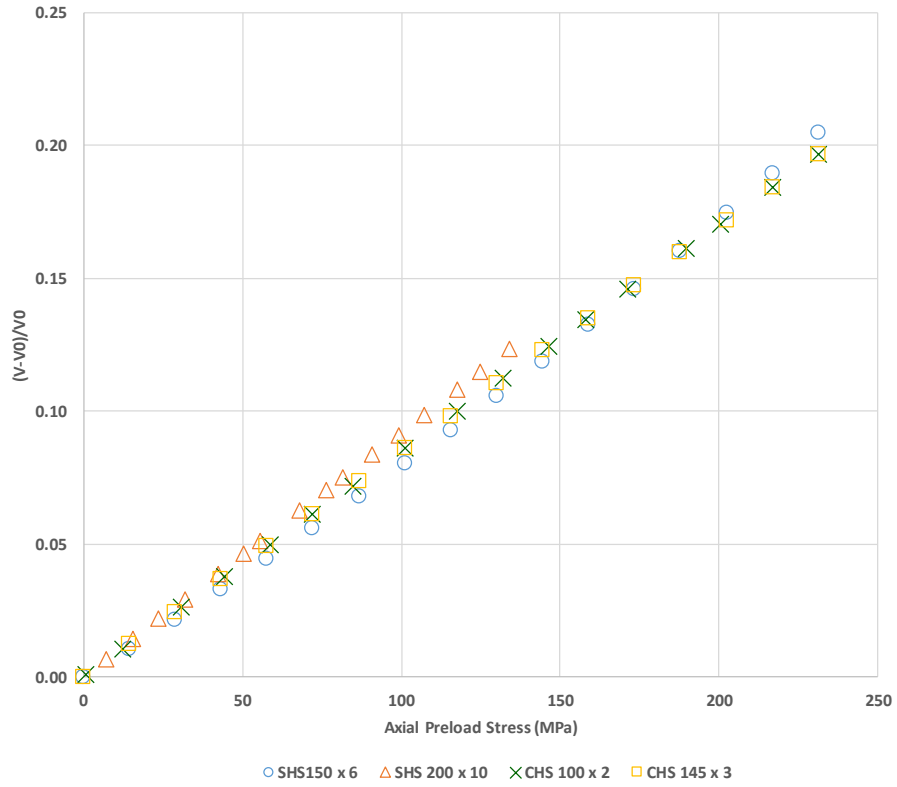


Figure 12 – Comparison of Acoustoelastic Constants for Various Sections

Table 5 – Results for Experimental Acoustoelastic Constants

Specimen	K (MPa ⁻¹)	R ²
SHS 150 x 6	8.48×10^{-4}	0.995
SHS 200 x 10	9.20×10^{-4}	1
CHS 100 x 2	8.50×10^{-4}	1
CHS 145 x 3	8.50×10^{-4}	1

Numerical Validation

The finite element model was constructed in ABAQUS [8] for a two-dimensional planar model consisting of the wedges and the specimen, with the transmitter probe ($f = 5\text{MHz}$) represented by a force-time function, $F(t)$, shown in Equation 7[17] for, and the receiver probe simplified to a probe point to monitor the incident ultrasonic signals, and shown schematically in Figure 13.

$$F(t) = \left[1 - \cos\left(\frac{2\pi ft}{3}\right) \right] \cdot \cos(2\pi ft)$$

Equation 7



Figure 13 – Outline of the Numerical Model

The plane specimen thickness of 100mm x 10mm is used to simulate the wave propagation under the excitation function defined earlier, with the boundary condition and initial stress, as shown in Figure 13. The CPE4R plane strain element with reduced integration is used to model the specimen and the wedge. The wedges are idealised with straight bottom faces, instead of the curved faces which was used in the experiment to reflect the actual set position of the curved faced wedge in the final position before being strapped with wires around the steel specimen. In both cases, the signal will be allowed to pass through the wedge into the steel specimen at its point of contact, therefore justifying this step in the numerical modelling. The ultrasonic signal is modelled with the amplitude generated from Equation 7 by prescribed nodal displacements. The residual compressive stresses are applied at the free edges of the specimen, and are set from 10MPa to 1000MPa.

The explicit analysis was carried out to simulate the propagation of the ultrasonic waves, particularly the LCR component under compressive residual stress conditions imposed onto the specimen by means of the initial stress input, σ under elastic material considerations. The sequence of wave travel in the specimen is shown in Figure 14 in terms of induced stress on the specimen, showing the predominantly LCR wave components reaching the receiver wedge ahead of the shear components or the reflected wave from the specimen boundary. The individual wave components (LCR and shear components) are distinctively shown in Figure 15, transmitted by the particles in the medium oscillating normally or in-line with these waves respectively.

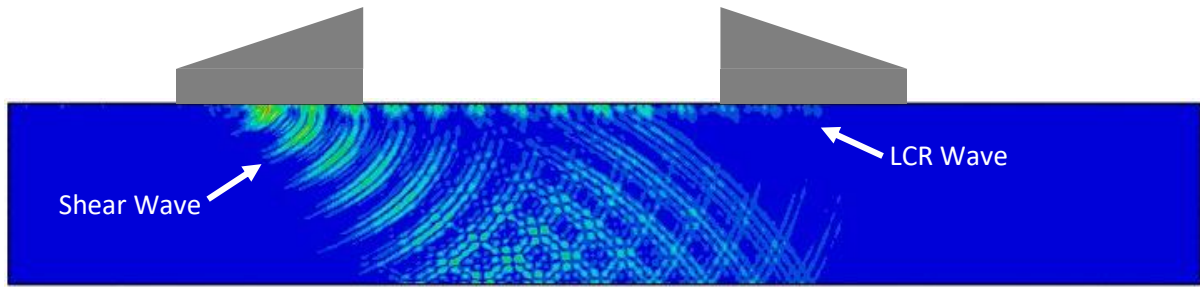


Figure 14 – Numerical Result Contour for Pressure Induced by Wave Propagation

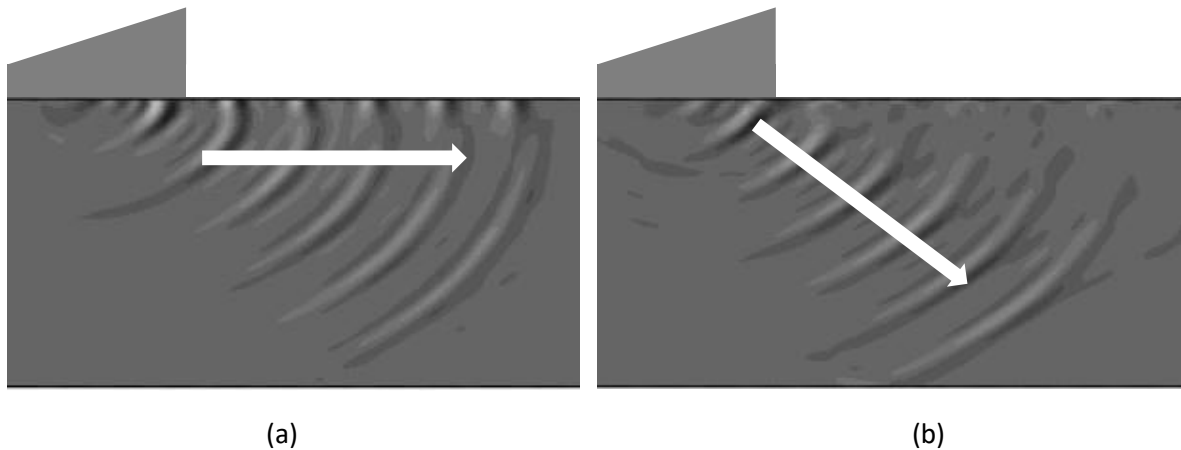
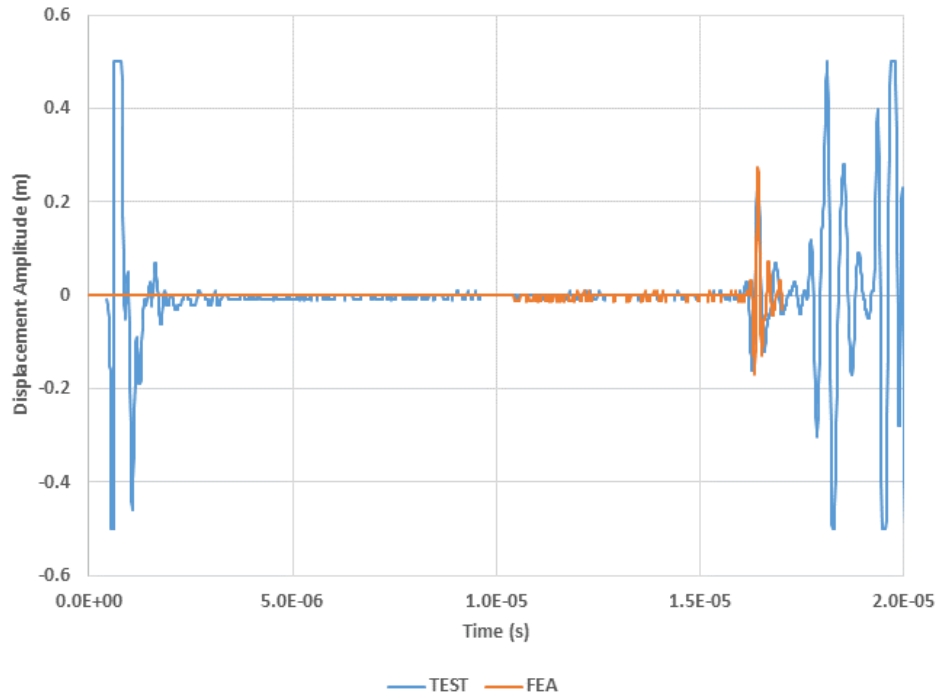
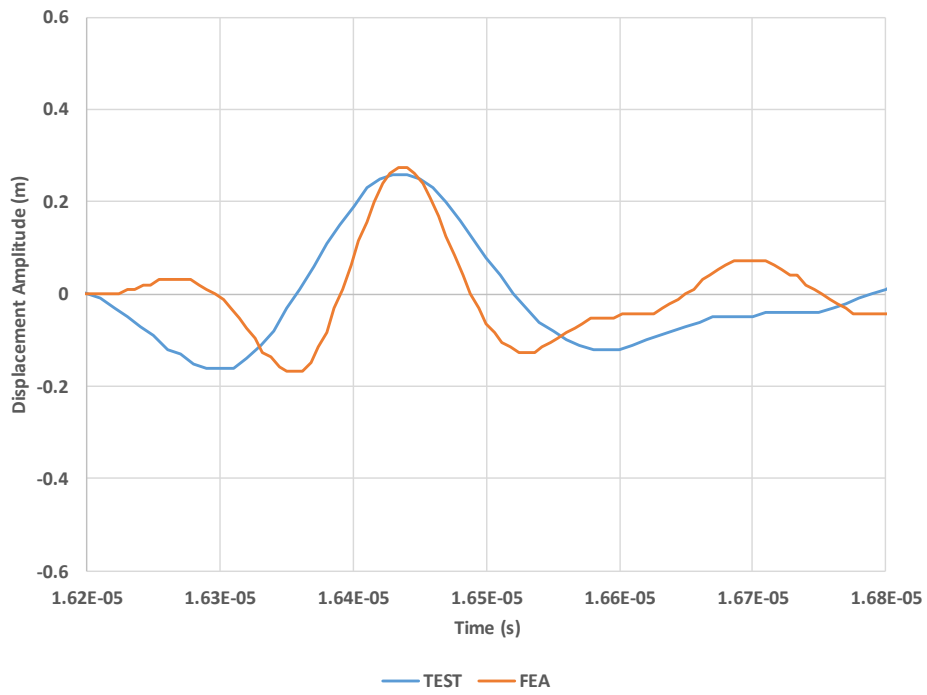


Figure 15 – (a) LCR Wave, and (b) Shear Wave Components in the Specimen

The measurement of the time taken for the LCR wave to travel from the bottom of the transmitter wedge to the incident point at the bottom of the receiver wedge is measured for each stressed condition, and the resulting calibration curve can be plotted. The plot shown in Figure 16 compares the FEA obtained wave forms to that obtained from the test for the 10mm thick specimen under 200MPa preload axial stress, along with a close-up view to highlight the variation between the LCR peaks at receiver probing point. The resulting acoustoelastic calibration curve are also shown for the FEA verification, and compared against the previously obtained curve from the test. A small deviation is observed for the higher stresses applied, as the test is limited to the elastic bounds of the specimen material whilst the analysis can be extended further to visualise any prominent response which could be missed during the test. The acoustoelastic constant of about $9.13 \times 10^{-4} \text{ MPa}^{-1}$ ($R^2 = 99.74\%$) is evaluated from the linear fit slope, and comparing against Table 5 shows a 7% deviation and remains within acceptable tolerances. The LCR wave speed is also measured to be approximately 5986m/s and is within acceptable limit of the measured nominal value of 5939m/s in an unstressed specimen state. The measured shear wave angle to the vertical in measured from the model to be approximately 33.7° , as compared to the 32.3° calculated from Snell's law.



(a)



(b)

Figure 16 – Comparison of FEA and Test for 200MPa case on 10mm Thick Specimen Showing (a) Overview of Recorded Wave Form, (b) Zoom-In of The Wave Peaks of Interest

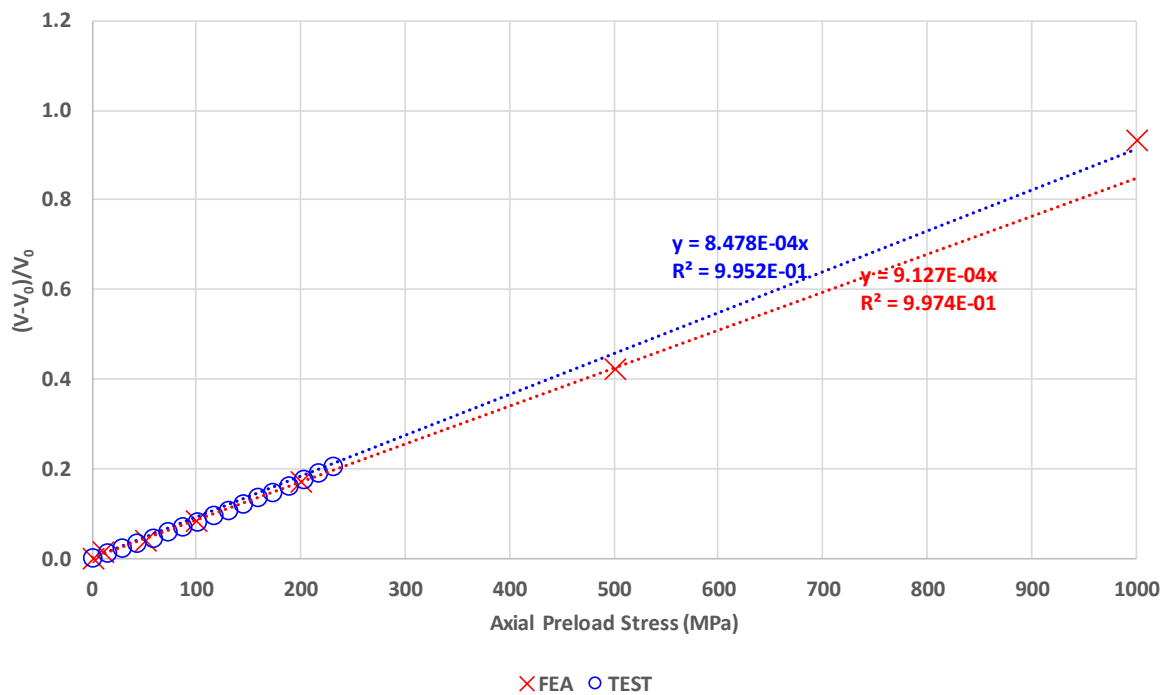


Figure 17 – Comparison of FEA and Test for Obtained Acoustoelastic Calibration Curve

IMPLEMENTATION FOR IN-SITU OFFSHORE CONDUCTOR MEASUREMENT

The technique of using the ultrasonic based LCR wave to measure the conductor preloads or the residual construction loads has been demonstrated in a laboratory based experimental work, and numerical analyses. This establishes its applicability in the integrity screening and assessments of ageing platform conductors mainly in the mature shallow water fields worldwide, and provides an instrument to perform effective prioritisation of conductors which really need repairing, from those with remaining structural resistance for continued service.

Several factors need to be considered to package this technique for in-situ measurements in the offshore fields. The prime importance is to ensure the system as being safe to operate in an explosive environment of the oil platforms, and complying to requirements of operator company safety policies. Portability and lightweight construction is also crucial to ensure ease-of-use for any technical personnel. A portable version of this setup is necessary, which means that the wedge need to be integrated to a hand-held device to a design shown in Figure 18. The wedge is replaced with an integrated handheld PMMA/plexi unit which mounts the probes with a constant pressure to enforce contact onto the conductors and the measurement software is set to run within an android device (or tablet unit), connected to the ultrasonic box. The software is also customised to conveniently produce the preload value based on the input of acoustoelastic constant as determined from the laboratory tests. Prior to measurements of a specific field, laboratory tests on sample steel from the conductor materials will need to be tested to determine the precise acoustoelastic constant for use during in-situ measurements. However, due to the standard practice of having the same drilling contractor to drill all the wells within the oil field, and adhering to the same well design and material specifications, it is generally accepted that one specimen should suffice, as the maximum difference in evaluated preload stresses is within 10% and can be tolerated.

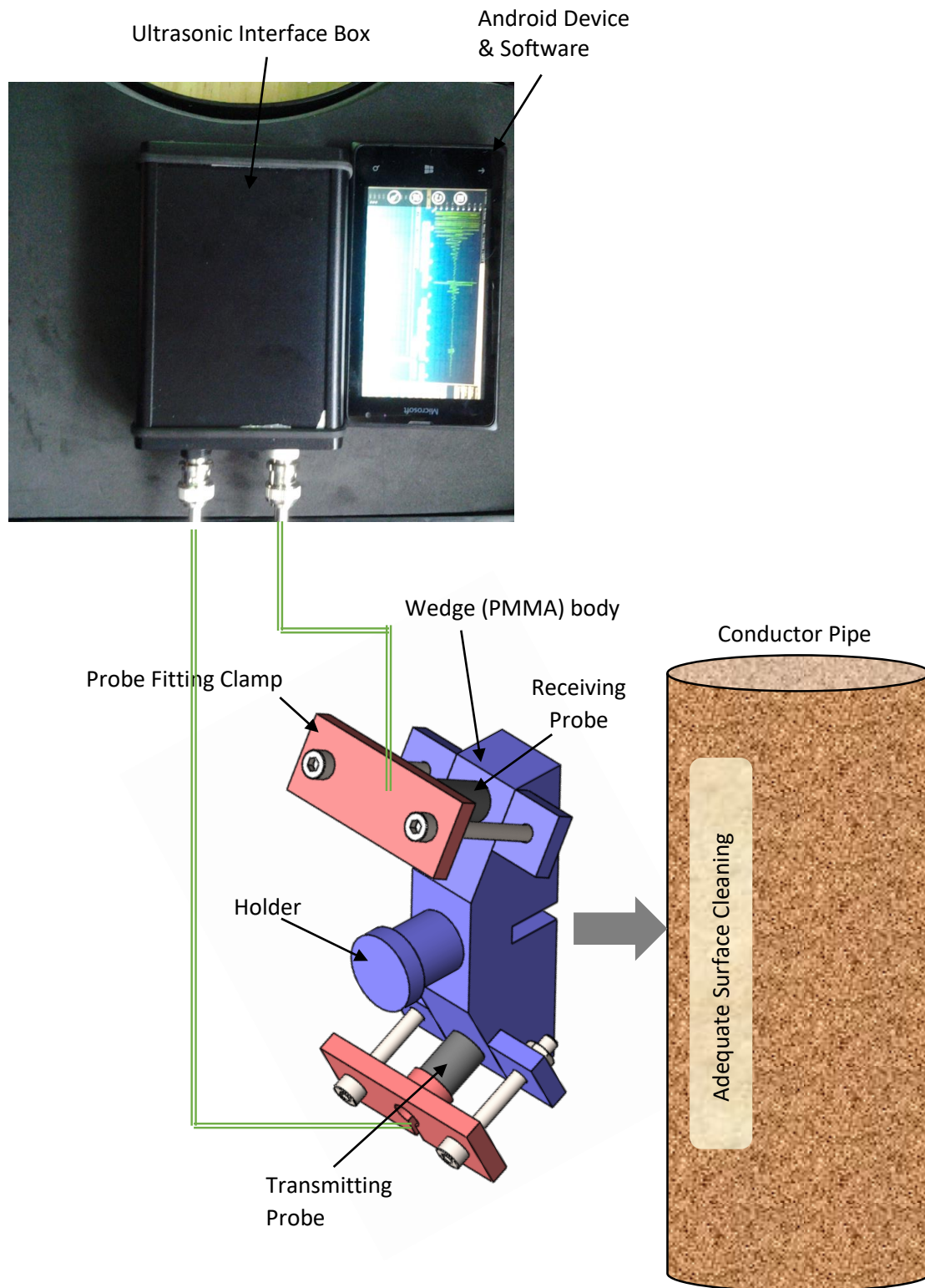


Figure 18 – Portable and Integrated Measurement System

The generic workflow for offshore in-situ measurement is presented in Figure 19. Upon selecting the candidate ageing wells for integrity screening, a preliminary assessment is necessary to determine if these wells are suited for life extension based on visual inspections for signs of collapse/damage, or by carrying out preliminary structural assessments to obtain remaining structural resistance. A sample material is ideally required to carry out laboratory calibration of the acoustoelastic constant which will

consider effects of material qualities, compositions and other parameters. Alternatively, numerical analysis can be carried out to determine the preliminary approximation of the constant. This is followed by the in-situ measurement of the TOF on the conductors, preferably right below the wellhead flange to obtain the maximum preloads. Presence of severe corrosion flakes and thick coating may affect the readings, and must be removed by light sanding, just sufficient to create a smooth surface for the probe contact points. Unlike strain gauging technique, there is no need for grinding to expose bare metal for accurate reading, as the LCR wave is a subsurface wave travelling beneath the outer layer. The preload value can then be included in to the stress calculations and checked against remaining resistance prior to any necessary repair decisions.

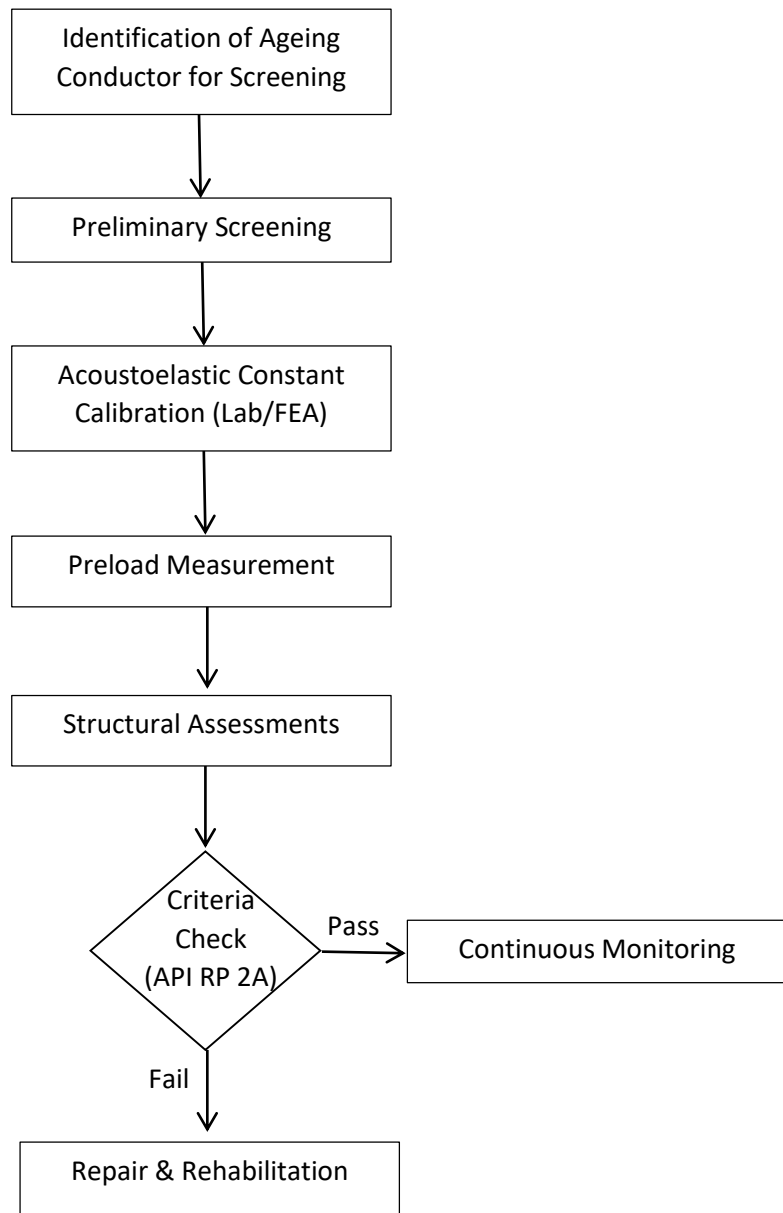


Figure 19 – Workflow for In-Situ Measurement

SUMMARY AND CONCLUSION

Integrity assessment and life extension of ageing wells are an important part of operator's activities worldwide, in maintaining their good producer wells, whilst keeping costs low in a non-performing economic climate. The structural elements of these wells, consisting primarily of the conductor and casing strings experience severe corrosion and the subsequent in-place assessments are critical in identifying wells requiring repairs and rehabilitations. Stress analyses can be carried out considering the environmental loads, equipment weights and the well construction loads, or preloads which remains in the well from the drilling stage. The axial preload makes up about 70% of the component which contribute towards the total stress at the splash zone region, and the remaining 30% comes from the environmental bending, making it a critical aspect in assessments of ageing well conductors. Conventional assessments show over-conservative stresses on the conductor, and unnecessary repairs may need to be carried out, with costs and resources indirectly proportional to water depths and metocean conditions at the field location.

This paper presents the application of ultrasonic based non-destructive method to efficiently measure the existing preload on the conductors (and casings, with available access) implementing the acoustoelastic technique by measuring the TOF of the ultrasonic wave, and to predict the existing stresses based on a laboratory calibrated material constant, or acoustoelastic constant. The setup of the system in a laboratory environment is carried out under a compression test machine to impart increments of compressive stresses, and the TOF is evaluated at each stress increment resulting in the calibration curves for various shapes and sizes of Grade-B steel. This is confirmed by numerical analyses using the finite element method to verify the magnitude order of the acoustoelastic constant, and to visually observe the wave propagation and their distinctive properties. This enables further analyses to be carried out to design a more portable and automated measurement system for use on aged offshore platforms.

In conclusion, this paper develops and highlights the potential of using the ultrasonic based acoustoelastic method on aged well conductors to determine the preloads, which inherently represents the cement state, downhole integrity of the casing strings and soil bearing effectiveness. The reliable measurement of the preload by this method can help reduce, if not eliminate, the unnecessary over-conservatisms in integrity assessment of aged well conductors towards crude production sustainability with existing assets. Further global stress analyses on the conductor system, with the measured preload values can help prioritise the conductors which critically need to be repaired, from those that have remaining adequate structural resistance.

ACKNOWLEDGEMENT

The authors would like to thank the academic support from the University of Malaya (Malaysia), and to Azakti Energy Ltd (United Kingdom) for the funding and equipment used in this research as part of their joint industry-university collaboration in the development of novel offshore integrity inspection technologies.

REFERENCES

- [1] Ramasamy, R., Aljaberi, M. S., & Junaibi, H. A. (2014). Ageing Offshore Well Structural Integrity Modelling, Assessment and Rehabilitation. Abu Dhabi International Petroleum Exhibition and Conference. doi:10.2118/171741-ms.
- [2] S. Talabani, B. Atlas, M.B Al-Khatiri, M.R. Islam, An Alternate Approach to Downhole Corrosion Mitigation, *J. Petroleum Science and Engineering*, 26 (2000), 41–48.
- [3] The Institute of Petroleum, London – “Guidelines for the Analysis of Jackup and Fixed Platform Well Conductor Systems”. July 2001
- [4] B. Stahl, M.P. Baur, Design Methodology for Offshore Platform Conductors, Offshore Technology Conference, 5/5/1980, Houston, Texas, 1980, OTC-3902-MS.
- [5] API – “Recommended Practice for Planning, Designing and Constructing Fixed Offshore Platforms”. API-RP-2A WSD, 21st Edition, December 2000.
- [6] API – “Specifications for Casings and Tubings”. API-SPEC-5CT, 8th Edition, July 2005.
- [7] Ramasamy, R., Ibrahim, Z., Suhatri, M. Criticality of Conductor/Casing Integrity for Ageing Offshore Well Life Extension, Regional Marine and Mechanical Engineering Conference (ReMME), Malaysia, October 2016, Paper-16.
- [8] Abaqus Theory Manual, Version 6.11, 2011.
- [9] Amleh, L. “Bond deterioration of reinforcing steel in concrete due to corrosion”, PhD Thesis, McGill University, 2000.
- [10] Yuan, Zhaoguang, Paolo Gardoni, Jerome Schubert, and Catalin Teodoriu. "Cement Failure Probability Analysis in Water Injection Well." *Journal of Petroleum Science and Engineering* 107 (2013): 45-49.
- [11] Crecraft, D. (1968). Ultrasonic measurement of stresses. *Ultrasonics*, 6(2), 117-121. doi:10.1016/0041-624x(68)90205-9.
- [12] Liu, S., Pan, Q., Xu, C., & Xiao, D. (2015). Calculation Techniques of two-dimensional residual stress field for mechanical engineering application. *Proceedings of the International Conference on Computer Information Systems and Industrial Applications*. doi:10.2991/cisia-15.2015.165.
- [13] Acoustoelasticity using longitudinal waves for residual stress evaluation. (1995). *NDT & E International*, 28(2), 118. doi:10.1016/0963-8695(95)93327-3.
- [14] Srinivasan, M. N., Joshi, S., & Zhou, J. (2012). Development of a Numerical Model to Predict Residual Stress Based on Acoustoelastic Effect Using Critically Refracted Ultrasonic Longitudinal (LCR) Waves. Volume 12: *Vibration, Acoustics and Wave Propagation*. doi:10.1115/imece2012-89146
- [15] Yuan, Maodan; Kang, To; Kim, Hak-Joon; Song, Sung-Jin (2011). A Numerical Model for Prediction of Residual Stress Using Rayleigh Waves: *Journal of Korean Society for Non-Destructive Testing*, Vol. 31, No. 6 (2011. 12).
- [16] K. Graff, “Wave Motion in Elastic Solids”, Dover Publications, New York, 1978.
- [17] Baskaran, G., Rao, C. L., & Balasubramaniam, K. (2007). Simulation of the TOFD technique using the finite element method. *Insight - Non-Destructive Testing and Condition Monitoring*, 49(11), 641-646. doi:10.1784/insi.2007.49.11.641.